WIRELESS COMMUNICATIONS AND MOBILE COMPUTING
Wirel. Commun. Mob. Comput. (2011)
Published online in Wiley Online Library (wileyonlinelibrary.com). DOI: 10.1002/wcm.1093

RESEARCH ARTICLE

Sequential frequency reuse with power control for OFDMA systems

Bumkwi Choi, Seyoun Lim and Tae-Jin Lee*

School of Information and Communication Engineering, Sungkyunkwan University, Suwon, 440-746, South Korea

ABSTRACT

Orthogonal frequency division multiple access (OFDMA) is a promising technique for high data rate communications in future cellular systems. Since frequency resources are universally reused in every cell in a system, a typical OFDMA system tries to maximize the spectral efficiency. Users located near the cell-edge tend to have the weakest signal strength. So they might experience severe inter-cell interferences (ICIs). In this paper, we propose a sequential frequency reuse (SqFR) that reduces ICIs by a sequential sub-channel allocation. By giving more power to sub-carriers allocated to cell-edge users, our SqFR significantly enhances the performance of cell-edge users. The performance of the proposed SqFR is investigated via the analysis and simulations. Simulation results show that proposed SqFR improves the performance of cell-edge users in an OFDMA system under both homogeneous and heterogeneous traffic conditions. Copyright © 2011 John Wiley & Sons, Ltd.

KEYWORDS

frequency reuse; interference coordination; OFDMA; sub-channel allocation

***Correspondence**

Tae-Jin Lee, School of Information and Communication Engineering, Sungkyunkwan University, Suwon, 440-746, South Korea
E-mail: tjlee@ece.skku.ac.kr

1. INTRODUCTION

Orthogonal frequency division multiple access (OFDMA) has come into the spotlight for the broadband wireless multiple access technology in the next generation cellular systems, e.g., Worldwide Interoperability for Microwave Access (WiMAX) [1] and 3GPP Long Term Evolution (LTE) [2]. Since OFDMA is a multi-user version of orthogonal frequency division multiplexing (OFDM), it has advantages to cope with various channel conditions, e.g., narrowband interference, and frequency-selective fading due to multipath. In OFDMA systems high-rate serial data streams are divided into several parallel low-rate data streams one for each sub-channel (carrier), and the closely-spaced orthogonal sub-carriers simultaneously carry data. The low symbol rate makes the use of a guard interval between symbols affordable, being able to handle time-spreading and eliminate intersymbol interference (ISI) [3,4].

In OFDMA systems the spectral efficiency can be increased by adaptive modulation and coding (AMC) [5]. AMC provides the adaptability to match the modulation-coding scheme with the received signal quality, e.g., signal-to-interference-plus-noise ratio (SINR). In a system with AMC, users close to the base station (BS) are generally assigned higher order modulation scheme with higher code rates, but the modulation order and code rate tend to decrease when users are located at the cell-edge area.

Since typical OFDMA systems have frequency reuse factor (FRF) of 1, i.e., a whole frequency bandwidth is reused in every cell of a system, users near the cell-edge might experience inter-cell interference (ICI). To overcome the ICI problem, fractional frequency reuse (FFR) has been introduced [6]. As depicted in Figure 1, FFR divides the whole frequency bandwidth into two reserved parts: cell-edge bandwidth, and cell-center bandwidth for cell-edge users and cell-center users, respectively. The cell-center bandwidth is reused in every cell while the cell-edge bandwidth is partially reused. The ratio of the cell-center bandwidth to the whole frequency bandwidth determines the amount of the cell-center bandwidth. By assigning orthogonal cell-edge bandwidth to each of cells, FFR can increase the performance of cell-edge users. Furthermore, the adaptive sub-carrier allocation can enhance the performance of cell-edge users [7,8].

In References [9–11], FFR for Mobile WiMAX is considered, which suggests time division of the available total bandwidth with different FRFs, i.e., cell-edge bandwidth with FRF of 3 and cell-center bandwidth with FRF of 1. So, downlink subframe is split into two parts: one for

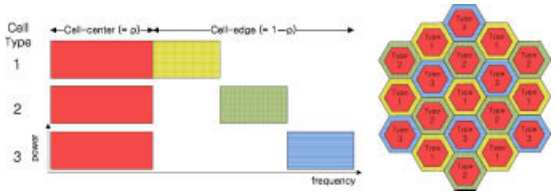

Fig. 1. An example of the typical FFR.

cell-center users, and the other for cell-edge users. While the whole frequency bandwidth can be assigned to cell-center users during the first part of the subframe, only a fraction of the bandwidth is assigned to cell-edge users during the second part of the subframe, which may not fully utilize the bandwidth. In References [12] and [13], the client-centric FFR based on user cooperation has been proposed. In this decentralized FFR, users at the cell-edge in a system have cooperative connectivity among nearby users to sense their environments and exchange their channel quality indicator (CQI) with the objective of finding viable sub-channel allocations. Since the interference mitigation is performed through cell-edge users rather than through the coordination among BSs, mobile stations might face power-consumption problem. In Reference [14], an analysis of the theoretical capacity of an OFDMA cellular system in a multi-cell environment has been introduced. It calculates SINR of a user with a given traffic load of a cell. In OFDMA, however, one or more sub-carriers can be allocated independently to a user. So SINR needs to be calculated for a sub-carrier.

In this paper, we focus on the frequency partitioning mechanism and interference mitigation method without channel state information (CSI) and propose a sequential frequency reuse (SqFR) with power control for OFDMA systems. The proposed SqFR utilizes the whole frequency bandwidth and can avoid serious ICIs from neighboring cells by providing cell-specific sub-channel allocation to each cell. In addition, by giving more power to sub-carriers for cell-edge users, one can increase carrier-to-interference-plus-noise ratio (CINR) of cell-edge users. The organization of the paper is as follows. The proposed SqFR is described in Section 2. In Section 3, we analyze the total cell capacity to evaluate the performance of the proposed SqFR. We simulate our proposed SqFR and verify the analysis in Section 4. Finally, we make a conclusion in Section 5.

2. PROPOSED SEQUENTIAL FREQUENCY REUSE

In this section, we describe the proposed SqFR. We present the frequency partitioning mechanism and the sub-channel allocation policy of SqFR.

2.1. Frequency partitioning mechanism

We propose SqFR as an efficient frequency reuse scheme to increase the capacity of cell-edge users with little sacrifice of the total cell capacity in OFDMA systems. Since each cell has FRF of 1 in our SqFR, each cell can use the whole frequency spectrum in a system. In SqFR, all sub-carriers are indexed from 0 to $N_{\text{subc}}-1$, where N_{subc} is the number of total sub-carriers in a system. When a system has M cell patterns, sub-carriers are partitioned into M sub-channel sets as follows:

$$F_i = \{f_k | i\alpha \le k \le (i+1)\alpha - 1\}, \quad 0 \le i \le M-1 \tag{1}$$

where f_k is the kth sub-carrier, F_i is the ith sub-channel set, and $\alpha = \lfloor \frac{N_{subc}}{M} \rfloor$. The function $\lfloor x \rfloor$ denotes the largest integer which is less than or equal to x. Finally each sub-channel set is further partitioned into M segments. So each segment in the sub-channel set is described as

$$S_{i,j} = \{f_k | i\alpha + j\beta \le k \le i\alpha + (j+1)\beta - 1\},$$
$$0 \le i \le M-1, \quad 0 \le j \le M-1 \tag{2}$$

where $\beta = \lfloor \frac{\alpha}{M} \rfloor$. These segments in the sub-channel sets are grouped into two different classes, C^i_{edge} and C^i_{center}, which are the set of sub-carriers that are allocated to cell-edge users and cell-center users of type i, respectively,

$$C^i_{\text{edge}} = \{S_{i \bmod M,i}, S_{(i+1) \bmod M,i}, \cdots, S_{(i+M-1) \bmod M,i}\},$$
$$C^i_{\text{center}} = F - C^i_{\text{edge}}, \qquad 0 \le i \le M-1, \tag{3}$$

where $i \bmod M$ is modulo M operation on i, and the set F is

$$F = \{f_k | 0 \le k < N_{\text{subc}}\} \tag{4}$$

The floor functions in Equation (1) and Equation (2) may result in some remaining sub-carriers. The remaining sub-carriers are assigned to cell-center users to utilize all sub-carriers as in Equation (3). The transmission power of a sub-carrier for cell-edge users is ωP_0, where ω is the power amplification factor (PAF) and P_0 is the transmission power of a sub-carrier for cell-center users. By giving more power to the sub-carriers allocated to cell-edge users, we can increase CINR to support the quality of service for cell-edge users. The number of available sub-carriers assigned to cell-edge users is βM. As M increases, the number of sub-carriers assigned to cell-edge users decreases. So M should be carefully selected to accept sufficient cell-edge users in a system.

2.2. Sub-channel allocation policy

SqFR can avoid serious ICIs from neighboring cells by cell-specific sub-channel allocation. Let $Q_i, 0 \le i \le M-1$, denote the sequence type of the sub-channel allocation. Sub-channels of sequence type i are allocated to users by the

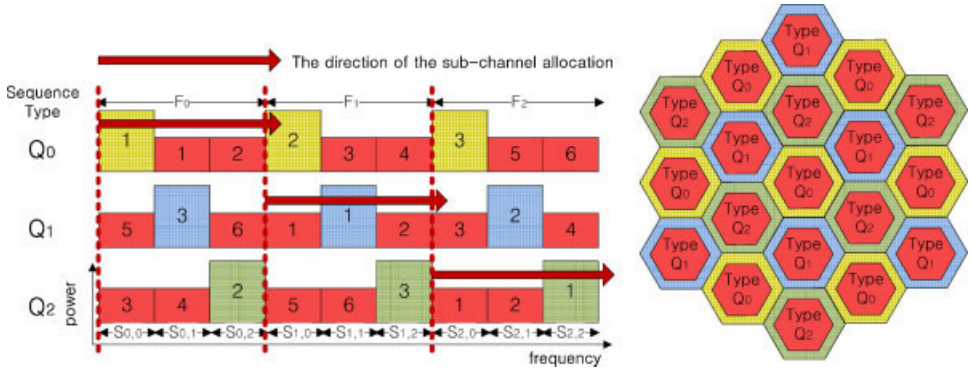

Fig. 2. An example of SqFR with the size of sub-channel sets, *M*, of 3.

following specific order:

$$Q_i = \begin{cases} S_{i \bmod M,i} \rightarrow S_{(i+1) \bmod M,i} \rightarrow \cdots \\ \rightarrow S_{(i+M-1) \bmod M,i}, \quad S_{i,j} \in C^i_{\text{edge}} \\ (F_{i \bmod M} - S_{i \bmod M,i}) \rightarrow \\ (F_{(i+1) \bmod M} - S_{(i+1) \bmod M,i}) \rightarrow \cdots \\ \rightarrow (F_{(i+M-1) \bmod M} - S_{(i+M-1) \bmod M,i}) \\ \rightarrow S_{\text{RS}}, \\ S_{i,j} \in C^i_{\text{center}} \end{cases} \tag{5}$$

where S_{RS} is the set of remaining sub-carriers.

Figure 2 shows an example of the proposed SqFR with the size of sub-channel sets, M, of 3. The system has three cell type and each cell type has the cell-specific sequential sub-channel allocation order. Each sub-channel set is represented as F_0, F_1, and F_2. And each segment is also represented as $S_{0,0}$, $S_{0,1}$, $S_{0,2}$, $S_{1,0}$, $S_{1,1}$, $S_{1,2}$, $S_{2,0}$, $S_{2,1}$, and $S_{2,2}$. The arrow shows the order of the sub-channel allocation of each sequence type. From Equation (5), the ordering of each sequence type in sub-channel allocation is

$$Q_0 = \begin{cases} S_{0,0} \rightarrow S_{1,0} \rightarrow S_{2,0}, \\ S_{0,1} \rightarrow S_{0,2} \rightarrow S_{1,1} \rightarrow S_{1,2} \rightarrow S_{2,1} \rightarrow S_{2,2} \\ \rightarrow S_{\text{RS}}, \end{cases}$$

$$Q_1 = \begin{cases} S_{1,1} \rightarrow S_{2,1} \rightarrow S_{0,1}, \\ S_{1,0} \rightarrow S_{1,2} \rightarrow S_{2,0} \rightarrow S_{2,2} \rightarrow S_{0,0} \rightarrow S_{0,2} \\ \rightarrow S_{\text{RS}}, \end{cases}$$

$$Q_2 = \begin{cases} S_{2,2} \rightarrow S_{0,2} \rightarrow S_{1,2}, \\ S_{2,0} \rightarrow S_{2,1} \rightarrow S_{0,0} \rightarrow S_{0,1} \rightarrow S_{1,0} \rightarrow S_{1,1} \\ \rightarrow S_{\text{RS}}. \end{cases}$$

For type Q_0 cell, when cell-edge users request resource, sub-carriers in $S_{0,0}$ are assigned preferentially to cell-edge users first. If all sub-carriers in $S_{0,0}$ are assigned to cell-edge users, sub-carriers in $S_{1,0}$ are allocated for incoming requests. Then, sub-carriers in $S_{2,0}$ begin to be allocated to cell-edge users when all sub-carriers in $S_{0,0}$ and $S_{1,0}$ have been allocated to cell-edge users. When cell-center users request resource, sub-carriers in $S_{0,1}$ are preferentially assigned to cell-center users and then if all sub-carriers in $S_{0,1}$ are assigned to cell-center users, sub-carriers in $S_{0,2}$,$S_{1,1}$,$S_{1,2}$,$S_{2,1}$, $S_{2,2}$, and the remaining sub-carriers are sequentially allocated to cell-center users. For type Q_1 and Q_2 cells, similar allocation policies are applied except the order of allocation of segments. SqFR with M of 4, illustrated in Figure 3, is not much different from SqFR with M of 3. The system with M of 4 has four cell types and the number of segments is larger than that of SqFR with M of 3. The frequency partitioning and the sub-channel allocation policy is almost the same as that of SqFR with M of 3.

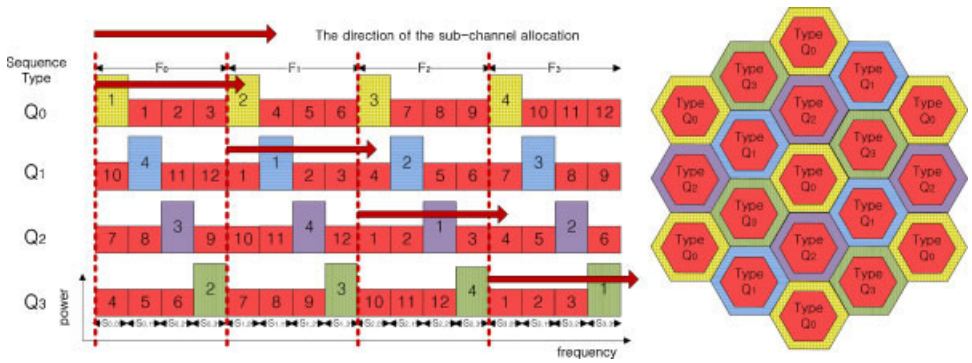

Fig. 3. An example of SqFR with the size of sub-channel sets, *M*, of 4.

3. ANALYSIS

In this section, we analyze the total cell capacity of a system with homogeneous and heterogeneous traffic.

3.1. Capacity analysis on homogeneous traffic

Under homogeneous traffic condition, we assume that every cell has the identical traffic distribution without small-scale fading and shadowing effect. Let $\gamma_{a,u,k}$ denote the instant CINR of user u in cell a for the kth sub-carrier. CINR $\gamma_{a,u,k}$ is represented as

$$\gamma_{a,u,k} = 10^{(P_{\text{tx}}+A_{\text{tx}}-P_{\text{pl}}(d_{a,u})+A_{\text{rx}}-P^{\text{int}}_{a,u,k})/10} \tag{6}$$

where P_{tx} (dBm) is the transmission power, A_{tx} and A_{rx} (dB) are the antenna gains of transmitter and receiver, respectively, $P_{\text{pl}}(.)$ (dB) is the path loss between the transmitter and the receiver, and $d_{a,u}$ (m) is the distance between user u in cell a and BS. When user u is in the cell-center region, the transmission power of the kth sub-carrier is P_0. When user u is in the cell-edge region, the transmission power is ωP_0. The interference signal power of user u in cell a from neighbor BSs for the kth sub-carrier, $P^{\text{int}}_{a,u,k}$, is

$$P^{\text{int}}_{a,u,k} = 10\log_{10}\left(\sum_{b\in U^{\text{int}}_{a,u}} c_{a,u,k,b}\cdot 10^{P^{\text{int}}_{a,u,k,b}/10} + 10^{N_{\text{noise}}/10}\right) \tag{7}$$

where $U^{\text{int}}_{a,u}$ is the universal set of interfering BSs to user u in cell a, and $c_{a,u,k,b}$ is the interference indicator that indicates whether the kth sub-carrier allocated to user u in cell a is simultaneously used in the neighbor cell b. So $c_{a,u,k,b}$ can be either 1 or 0 and is deterministic if the traffic loads of cells are the same, i.e., homogeneous traffic. The interference signal power from the neighbor BS b to user u in cell a, $P^{\text{int}}_{a,u,k,b}$, is

$$P^{\text{int}}_{a,u,k,b} = P_{tx} + A_{tx} - P_{pl}(d_{a,u,b}) + A_{rx}, \tag{8}$$

where $d_{a,u,b}$ is the distance between user u in cell a and the neighbor BS b. The noise power N_{noise} is

$$N_{\text{noise}} = \text{BW}\cdot N_{\text{thermal}} \tag{9}$$

where BW is the bandwidth of a sub-carrier, and N_{thermal} (dBm/Hz) is the thermal noise density.

The average capacity achieved by user u in cell a for the kth sub-carrier over the cell-area is given by

$$\tilde{C}_{a,u,k} = \frac{1}{A_{\text{cell}}}\cdot\int_{A_{\text{edge}}} \text{BW}\cdot\log_2(1+\gamma_{a,u,k})dA + \frac{1}{A_{\text{cell}}}\cdot\int_{A_{\text{center}}} BW\cdot\log_2(1+\gamma_{a,u,k})dA \tag{10}$$

where A_{cell} is the area of a cell, A_{edge} and A_{center} are the area of cell-edge and cell-center regions, respectively, and we use Shannon's channel capacity to calculate the capacity. The average capacity achieved by user u in cell a is, then, given by

$$\tilde{C}_{a,u} = n_{\text{subc}}\cdot\tilde{C}_{a,u,k} \tag{11}$$

where n_{subc} is the number of sub-carriers per user. Finally, the achievable capacity of cell a is given by

$$\tilde{C}_a = \sum_{u=1}^{N_{\text{MS}}}\tilde{C}_{a,u} \tag{12}$$

where N_{MS} is the number of users in cell a.

3.2. Capacity analysis on heterogeneous traffic

Under heterogeneous traffic condition, we assume that traffic loads of cells are independently and identically distributed (i.i.d.) uniform random variable. The traffic load is defined as the ratio of the number of active users to the number of total users in a cell. So the traffic load of each cell is independent and identically distributed (i.i.d.). Then, the interference indicator from Equation (7) is no more deterministic. The interference indicator, $c_{a,u,k,b}$, is now modeled by a Bernoulli random variable and is represented as

$$c_{a,u,k,b} = \begin{cases} 1, & \text{if BS } b \text{ uses the same } k\text{th sub}-\text{carrier as BS } a \\ 0, & \text{otherwise.} \end{cases} \tag{13}$$

The probability mass function (pmf) of $c_{a,u,k,b}$ is given by

$$\begin{aligned} P[c_{a,u,k,b}=1] &= p^{Q_i}_{a,u,k,b}, \\ P[c_{a,u,k,b}=0] &= 1-p^{Q_i}_{a,u,k,b}, \end{aligned} \tag{14}$$

where $p^{Q_i}_{a,u,k,b}$ is the probability that the kth sub-carrier allocated to user u in cell a is simultaneously used in the neighbor BS b that has the sequence type Q_i.

In order to calculate the interference signal power from neighbor BSs, we consider every possible set of interfering neighbor BSs. Hence, we define a universal set of interference indicator vectors for the kth sub-carrier, $U_{\vec{C}_k}$, as

$$U_{\vec{C}_k} = \left\{\vec{C}_k | \vec{C}_k = \left(x_{a,u,k,1}, x_{a,u,k,2}, \cdots, x_{a,u,k,b}, \cdots x_{a,u,k,N_{\text{BS}}}\right),\quad x_{a,u,k,b}\in\{0,1\}\right\}, \tag{15}$$

where $\vec{C}_k$ is the interference indicator vector, and N_{BS} is the number of total interfering BSs. The pmf of $\vec{C}_k$ is

$$P[\vec{C}_k = \vec{c}_k] = P[c_{a,u,k,1} = x_{a,u,k,1}, c_{a,u,k,2} = x_{a,u,k,2}, \cdots, c_{a,u,k,N_{\text{BS}}} = x_{a,u,k,N_{\text{BS}}}]$$

$$= \prod_{b \in U_{a,u}^{\text{int}}} P[c_{a,u,k,b} = x_{a,u,k,b}]$$

$$= \prod_{b \in U_{a,u}^{\text{int}} \text{and} c_{a,u,k,b}=1} p_{a,u,k,b}^{Q_i} \times \prod_{b \in U_{a,u}^{\text{int}} \text{and} c_{a,u,k,b}=0} (1 - p_{a,u,k,b}^{Q_i}) \quad (16)$$

We consider SqFR with M of 3 to find $p_{a,u,k,b}^{Q_i}$. We assume that a target cell, which is the designated cell to calculate the capacity, has sequence type Q_0 and only one sub-channel, which consists of n_{subc} sub-carriers, is allocated to each user. We define $N_{\text{edge}}^{\text{subch}}$ and $N_{\text{center}}^{\text{subch}}$ as the number of total sub-channels for cell-edge and cell-center users, respectively, and N_{seg} as the number of sub-carriers in a segment. Since sub-channels are allocated sequentially from the first sub-channel set, sub-channels located in the first sub-channel set are interfered more than those in the second or the third sub-channel sets. Therefore, $p_{a,u,k,b}^{Q_0}$ in F_0 is higher than that in F_1, and $p_{a,u,k,b}^{Q_0}$ in F_1 is higher than that in F_2. Similarly, $p_{a,u,k,b}^{Q_1}$ in F_1 is higher than that in F_2 and F_0, and $p_{a,u,k,b}^{Q_2}$ in F_2 is higher than that in F_0 and F_1.

Since the traffic load of each cell is a discrete uniform random variable and only one sub-channel is allocated to each user, the number active cell-edge and cell-center users can be from 0 to $N_{\text{edge}}^{\text{subch}}$ and from 0 to $N_{\text{center}}^{\text{subch}}$, respectively. So there are total $N_{\text{edge}}^{\text{subch}} + 1$ possible cases for the traffic load of cell-edge region and $N_{\text{center}}^{\text{subch}} + 1$ possible cases for the traffic load of cell-center region. When the kth sub-carrier is in segment $S_{y,0}$, $0 \le y \le M-1$, $p_{a,u,k,b}^{Q_i}$ is computed as

$$p_{a,u,k,b}^{Q_i} = \frac{\frac{\tau_{Q_i} \cdot N_{Q_i}}{3} - \lfloor \frac{k-3 \cdot y \cdot N_{\text{seg}}}{n_{\text{subc}}} \rfloor}{N_{Q_i} + 1} \quad (17)$$

where N_{Q_i} and τ_{Q_i} are determined by the sequence type of the interfering BS b and the index of the sub-channel set where the kth sub-carrier is located. For $p_{a,u,k,b}^{Q_0}$, N_{Q_0} and τ_{Q_0} are

$$N_{Q_0} = N_{\text{edge}}^{\text{subch}}, \quad \tau_{Q_0} = \begin{cases} 3, & y = 0 \\ 2, & y = 1 \\ 1, & y = 2 \end{cases} \quad (18)$$

For $p_{a,u,k,b}^{Q_1}$,

$$N_{Q_1} = N_{\text{center}}^{\text{subch}}, \quad \tau_{Q_1} = \begin{cases} 1, & y = 0 \\ 3, & y = 1 \\ 2, & y = 2 \end{cases} \quad (19)$$

For $p_{a,u,k,b}^{Q_2}$, N_{Q_2}, and τ_{Q_2} are

$$N_{Q_2} = N_{\text{center}}^{\text{subch}}, \quad \tau_{Q_2} = \begin{cases} 2, & y = 0 \\ 1, & y = 1 \\ 3, & y = 2 \end{cases} \quad (20)$$

Similarly, when the kth sub-carrier is in segment $S_{y,1}$, $p_{a,u,k,b}^{Q_i}$ is represented as

$$p_{a,u,k,b}^{Q_i} = \frac{\frac{\tau_{Q_i} \cdot N_{Q_i}}{6} - \lfloor \frac{k-(3 \cdot y+1) \cdot N_{\text{seg}}}{n_{\text{subc}}} \rfloor}{N_{Q_i} + 1} \quad (21)$$

For $p_{a,u,k,b}^{Q_0}$, N_{Q_0}, and τ_{Q_0} are

$$N_{Q_0} = N_{\text{center}}^{\text{subch}}, \quad \tau_{Q_0} = \begin{cases} 6, & y = 0 \\ 4, & y = 1 \\ 2, & y = 2 \end{cases} \quad (22)$$

For $p_{a,u,k,b}^{Q_1}$,

$$N_{Q_1} = N_{\text{edge}}^{\text{subch}}, \quad \tau_{Q_1} = \begin{cases} 2, & y = 0 \\ 6, & y = 1 \\ 4, & y = 2 \end{cases} \quad (23)$$

For $p_{a,u,k,b}^{Q_2}$, N_{Q_2}, and τ_{Q_2} are

$$N_{Q_2} = N_{\text{center}}^{\text{subch}}, \quad \tau_{Q_2} = \begin{cases} 3, & y = 0 \\ 1, & y = 1 \\ 5, & y = 2 \end{cases} \quad (24)$$

Finally, when the kth sub-carrier is in segment $S_{y,2}$, $p_{a,u,k,b}^{Q_i}$ is

$$p_{a,u,k,b}^{Q_i} = \frac{\frac{\tau_{Q_i} \cdot N_{Q_i}}{6} - \lfloor \frac{k-(3 \cdot y+2) \cdot N_{\text{seg}}}{n_{\text{subc}}} \rfloor}{N + 1} \quad (25)$$

For $p_{a,u,k,b}^{Q_0}$, N_{Q_0}, and τ_{Q_0} are

$$N_{Q_0} = N_{\text{center}}^{\text{subch}}, \quad \tau_{Q_0} = \begin{cases} 5, & y = 0 \\ 3, & y = 1 \\ 1, & y = 2 \end{cases} \quad (26)$$

For $p_{a,u,k,b}^{Q_1}$,

$$N_{Q_1} = N_{\text{center}}^{\text{subch}}, \quad \tau_{Q_1} = \begin{cases} 1, & y = 0 \\ 5, & y = 1 \\ 3, & y = 2 \end{cases} \quad (27)$$

For $p_{a,u,k,b}^{Q_2}$, N_{Q_2}, and τ_{Q_2} are

$$N_{Q_2} = N_{\text{edge}}^{\text{subch}}, \quad \tau_{Q_2} = \begin{cases} 4, & y = 0 \\ 2, & y = 1 \\ 6, & y = 2 \end{cases} \quad (28)$$

Then the instant CINR of user u in cell a for the kth sub-carrier for $\vec{C}_k = \vec{c}_k$ is

$$\gamma_{a,u,k}^{\vec{c}_k} = 10^{(P_{\text{tx}} + A_{\text{tx}} - P_{\text{pl}}(d_{a,u}) + A_{\text{rx}} - P_{a,u,k}^{\text{int}}(\vec{c}_k))/10} \quad (29)$$

where $P_{a,u,k}^{\text{int}}(\vec{c}_k)$ is the interference signal power of user u in cell a for the kth sub-carrier from neighbor BSs for the

interference indicator vector $\vec{c}_k s$, which is represented as

$$P^{\text{int}}_{a,u,k}(\vec{c}_k) = 10\log_{10}\left(\sum_{b\in U^{\text{int}}_{a,u}} c_{a,u,k,b}\cdot 10^{P^{\text{int}}_{a,u,k,b}/10} + 10^{N_{\text{noise}}/10}\right) \quad (30)$$

where $P^{\text{int}}_{a,u,k,b}$ and N_{noise} are the same as in Equations (8) and (9).

We consider all possible interference scenarios to obtain the capacity of users. Let $\tilde{C}^{\text{inst}}_{a,u,k}$ denote the instant average capacity achieved by user u in cell a for the kth sub-carrier,

$$\tilde{C}^{\text{inst}}_{a,u,k} = \sum_{\vec{c}_k\in U_{\vec{C}_k}} \text{BW}\cdot\log_2(1+\gamma^{\vec{c}_k}_{a,u,k})\cdot P[\vec{C}_k=\vec{c}_k] \quad (31)$$

Then the average capacity achieved by user u in cell a for the kth sub-carrier over the cell-area is given by

$$\tilde{C}_{a,u,k} = \frac{1}{A_{\text{cell}}}\cdot\int_{A_{\text{edge}}}\tilde{C}^{\text{inst}}_{a,u,k}dA + \frac{1}{A_{\text{cell}}}\cdot\int_{A_{\text{center}}}\tilde{C}^{\text{inst}}_{a,u,k}dA \quad (32)$$

Finally, the achievable capacity of cell a is obtained by Equations (11) and (12).

4. PERFORMANCE EVALUATION

In this section, we present simulation results to evaluate the performance of the proposed SqFR and verify the analysis by simulations. We consider 19 cells (tier-1 and tier-2 cells) and the distance between BSs is 1 km. Users are uniformly distributed within each cell. Table I summarizes the simulation parameters. We use the modified COST-Walfish-Ikegami (WI) urban micro for non-line-of-sight (NLOS) outdoor path-loss model [15].

$$P_{\text{pl}}[dB] = 31.81 + 40.5\log_{10}(d[m]) \quad (33)$$

where d is the distance between a BS and a user.

Table I. Simulation parameters.

Parameter	Value
BS power	20 W
Radius of cells	577 m
Total frequency bandwidth in one cell	10 MHz
FFT size	1024
Number of data sub-carriers in one cell	768
Down-link symbol rate	9.76 ksymbols/s
Thermal noise density (N_{thermal})	−174 dBm/Hz
Antenna gains (A_{tx}, A_{rx})	0 dB
Shadowing standard deviation (σ)	8 dB

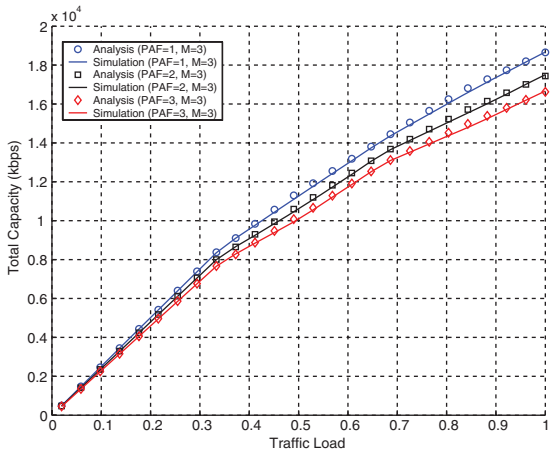

Fig. 4. Total capacity of a cell of the proposed SqFR with M of 3 under homogeneous traffic condition.

Figure 4 shows the total capacity of a cell of the proposed SqFR with M of 3 under homogeneous traffic condition. The bandwidth ratio between the cell-edge region and the cell-center region is 1:2 in the proposed SqFR with M of 3. Then the areas for each region, i.e., A_{edge} and A_{center}, are determined in proportion to the bandwidth to fairly allocate sub-carriers to users, i.e., A_{edge}: A_{center} = 1:2. Two transition points in the figure are due to the change of sub-channel sets from F_0 to F_1, and from F_1 to F_2. Since the traffic loads of cells in the system are identical, there are no ICIs from adjacent cells when the traffic load of a cell is below $\frac{1}{3}$, and ICIs from 2-tier cells are negligible. When the traffic load increases over $\frac{1}{3}$, ICIs from adjacent three cells start to appear. When the traffic load increases beyond $\frac{2}{3}$, ICIs from more cells begin to occur. So the slope of the capacity decreases as the traffic load of the cell increases. PAF plays a crucial role in the capacity. The more PAF we have, the less maximum total capacity we achieve. However, we can see later that the capacity of cell-edge users can be increased as PAF increases.

Figure 5 shows the total capacity of a cell of the proposed SqFR with M of 3 under heterogeneous traffic condition. Under heterogeneous traffic condition, all sub-channels have the probabilities of interference with one another. So, the transition points of the proposed SqFR may not be distinct. The maximum achievable capacity of a cell under heterogeneous traffic condition is greater than that under homogeneous traffic because the probability of interference is lower. Simulation results and analysis results are well matched for both homogeneous and heterogeneous traffic conditions.

To evaluate the performance of the proposed SqFR in a practical environment, we consider the Rayleigh fading channel. The multipath fading effect of the channel gain from a BS to a user is modeled as a second-order chi-square random variable with the mean of 1.0 [16]. we also consider the shadowing effect.

$$P_{\text{pl}}[dB] = 31.81 + 40.5\log_{10}(d[m]) + \chi_\sigma \quad (34)$$

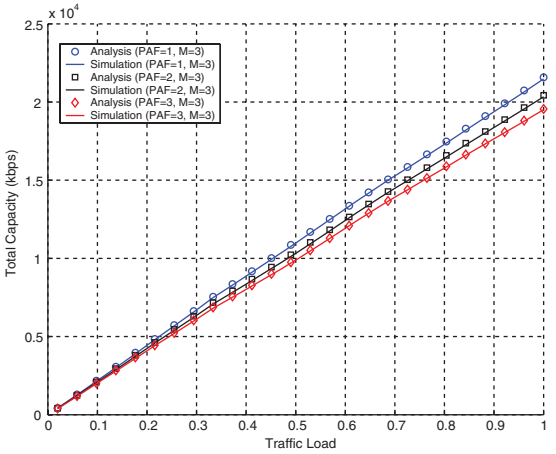

Fig. 5. Total capacity of a cell of the proposed SqFR with M of 3 under heterogeneous traffic condition.

Table II. Modulation and coding scheme (MCS) table.

CINR	Code rate	Modulation
−4.34	1/12	QPSK
−2.80	1/8	QPSK
−1.65	1/6	QPSK
0.31	1/4	QPSK
1.51	1/3	QPSK
4.12	1/2	QPSK
6.35	2/3	QPSK
9.50	1/2	16QAM
12.21	2/3	16QAM
13.32	1/2	64QAM
16.79	2/3	64QAM
20.68	5/6	64QAM

where χ_σ represents the outdoor shadowing (log-normal fading), which is characterized by the Gaussian distribution with zero mean and standard deviation σ. We use modulation and coding scheme (MCS) to calculate the throughput of a user. The reported CINR determines the modulation schemes and the code rate as shown in Table II [17]. We consider universal frequency reuse (UFR) which has FRF of 1 and the typical FFR with $\rho = 0.5$ to compare the performance of the proposed SqFR. The parameter ρ is the ratio of the cell-center bandwidth to the whole frequency bandwidth in FFR and can be chosen from 0 to 1.

In Figures 6 and 7, we evaluate the total throughput of a cell for three schemes under homogeneous traffic condition. The legend 'URF' denotes the universal frequency reuse and 'FFR' indicates the fractional frequency reuse. The legend 'SqFR' denotes our proposed sequential frequency reuse scheme. The proposed SqFR has better performance in low and medium traffic load. We observe critical points in the proposed SqFR, where the slope changes suddenly due to the additional interferences from other BSs by starting to use new sub-channels. In Figure 6, we can see two critical points of the proposed SqFR with M of 3, i.e., when the traffic load is around 0.33 and 0.66. When PAF varies from 3

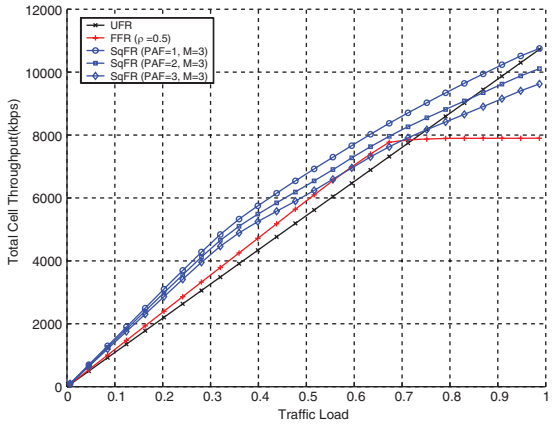

Fig. 6. Total throughput of a cell under homogeneous traffic condition for the proposed SqFR with M of 3, UFR, and FFR.

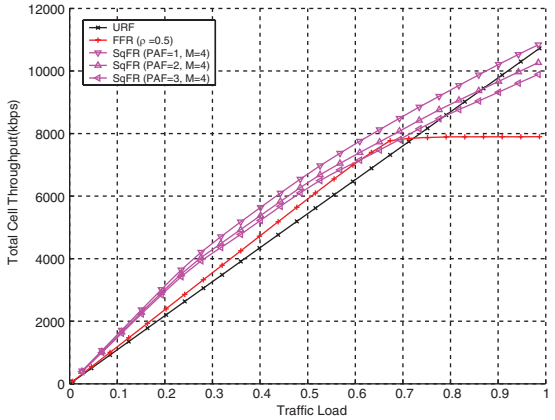

Fig. 7. Total throughput of a cell under homogeneous traffic condition for SqFR with M of 4, UFR, and FFR.

to 1, the proposed SqFR with M of 3 improves the throughput performance about 26–36% and 16–26% compared to that of UFR and FFR, respectively, when the traffic load is around 0.33. In Figure 7, we can see three critical points of the proposed SqFR with M of 4, i.e., when the traffic load is around 0.25, 0.50, and 0.75. When PAF varies from 3 to 1, the proposed SqFR with M of 4 improves the throughput performance about 32–42% and 21–30% compared to that of UFR and FFR, respectively, when the traffic load is around 0.25. The proposed SqFR with M of 4 shows better performace in terms of the maximum achievable cell throughput than that of the proposed SqFR with M of 3 as PAF increases since the frequency bandwith for cell-center users of the proposed SqFR with M of 4 is wider than that of the proposed SqFR with M of 3. In FFR, the total throughput is saturated when the traffic load is 0.66 because of the limited frequency bandwidth for cell-edge users.

Although the maximum achievable throughput of the proposed SqFR decreases a little as PAF increases, the throughput of cell-edge users drastically increases as shown in Figure 8. Thus, we observe a trade-off between the total cell throughput and the throughput of cell-edge users for

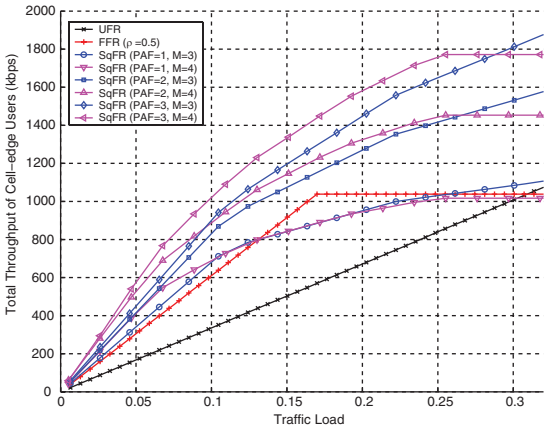

Fig. 8. Total throughput of cell-edge users under homogeneous traffic condition.

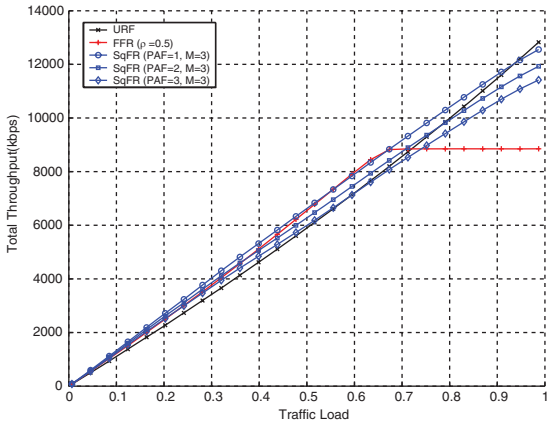

Fig. 9. Total throughput of a cell under heterogeneous traffic condition for SqFR with M of 3, UFR, and FFR.

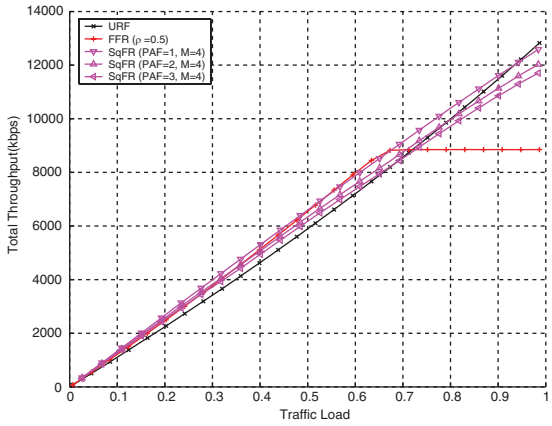

Fig. 10. Total throughput of a cell under heterogeneous traffic condition for SqFR with M of 4, UFR, and FFR.

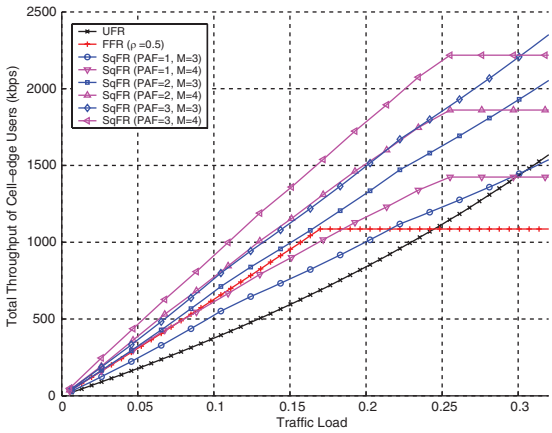

Fig. 11. Total throughput of cell-edge users under heterogeneous traffic condition.

varying PAF. As PAF increases, SqFR outperforms UFR and FFR. Moreover, the proposed SqFR with M of 4 performs better than the proposed SqFR with M of 3 since the transmission power on the sub-carrier of the proposed SqFR with M of 4 is higher than that of the proposed SqFR with M of 3.

Figures 9 and 10 demonstrate the total cell throughput of three schemes under heterogeneous traffic condition. Under heterogeneous traffic condition, the proposed SqFR has less performance gain than that under homogeneous traffic condition since every sub-channel has the possibility of being interfered. When the traffic load is around 0.33, the total throughput of a cell for the proposed SqFR with M of 3 in Figure 9 improves 8–18% over UFR as PAF varies from 3 to 1. As PAF varies from 3 to 1, the proposed SqFR with M of 4 in Figure 10 improves the throughput performance 11–18% over UFR. In addition, the proposed SqFR achieves the maximum cell throughput much greater than FFR since FFR has the limited frequency bandwidth. The total throughput of cell-edge users under heterogeneous traffic condition in Figure 11 presents similar trend as in Figure 8. The proposed SqFR significantly improves the total throughput of cell-edge users by increasing PAF.

Figure 12 shows the outage probabilities of three schemes when CINR_{out} is 0dB under homogeneous traffic. The outage probability is defined as

$$P_{\text{outage}}(\text{CINR}_{\text{out}}) = P[\text{CINR} < \text{CINR}_{\text{out}}] \qquad (35)$$

where CINR_{out} is a CINR threshold. Under homogeneous traffic, UFR and FFR has constant outage performance since ICIs from neighbor BSs are constant throughout the traffic load. The outage probability of SqFR, on the other hand, increases as the traffic load increases because of the sequential sub-channel allocation. At each transitional point, users experience additional ICIs from neighbor BSs. The figure demonstrates that our SqFR outperforms over UFR for all traffic load and over FFR in low and medium traffic load. As PAF increases, the outage performance of SqFR improves much better.

The outage probabilities of three schemes under heterogeneous traffic is shown in Figure 13. Unlike Figure 12, the outage performances of UFR and FFR improves as

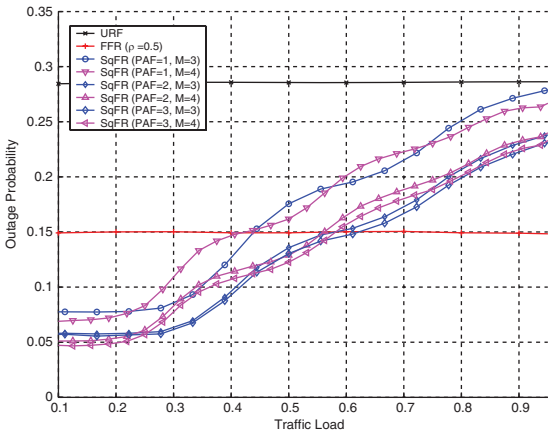

Fig. 12. Outage probability with $CINR_{out} = 0dB$ under homogeneous traffic condition.

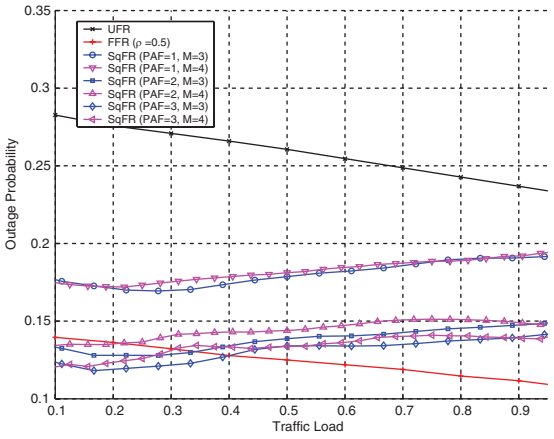

Fig. 13. Outage probability with $CINR_{out} = 0dB$ under heterogeneous traffic condition.

the traffic load increases since the sub-channels have less probability of being interfered under heterogeneous traffic condition. The outage performance of SqFR, however, slightly decreases as the traffic load increases since the sub-channels in the second and the third sub-channel sets have higher probabilities of interference than those in the first sub-channel set. As PAF increases, the outage performance of SqFR becomes close to that of FFR.

5. CONCLUSION

In this paper, we have proposed an efficient frequency reuse scheme, SqFR, for OFDMA systems. Giving more power to the sub-carriers allocated to cell-edge users, SqFR supports various quality-of-service requirements of cell-edge users. Moreover, by the cell-specific sequential sub-channel allocation, the proposed SqFR effectively reduces ICIs from adjacent cells. We have evaluated the performance of SqFR by analysis and simulations. Simulation results demonstrate that the proposed SqFR improves the throughput of cell-edge users and the outage performance under both homogeneous and heterogeneous traffic conditions of the system.

ACKNOWLEDGEMENTS

This research was supported by the MKE(The Ministry of Knowledge Economy), Korea, under the ITRC(Information Technology Research Center) support program supervised by the NIPA(National IT Industry Promotion Agency) (NIPA-2010–(C1090-1011-0005)).

REFERENCES

1. IEEE Standard for Local and Metropolitan Area Networks. Part 16: Air interface for fixed and mobile broadband wireless access systems. 2006; IEEE 2006.
2. 3GPP Technical Specification Group Radio Access Network. 3GPP TR 25.814 V1.0.2, Physical layer aspects for evolved UTRA (Release 7). 2006; 3GPP 2006.
3. Li G, Liu. H. Downlink radio resource allocation for multi-cell OFDMA system. *IEEE Transactions on Wireless Communications* 2006; **5**(12): 3451–3459.
4. Bodge M, Gross J, Wolfish A, Meyer M. Dynamic resource allocation in ofdm systems: an overview of cross-layer optimization principles and techniques. *IEEE Network* 2007; **21**: 53–59.
5. Kim J, Lee K-J, Sung CK, Lee. I. A simple SNR representation method for AMC schemes of MIMO systems with ML detector. *IEEE Transactions on Communications* 2009; **57**(10): 2971–2976.
6. Mobile WiMAX. Part I: A technical overview and performance evaluation. WiMAX Forum, March 2006.
7. Yan L, Wenan Z, Junde S. An adaptive subcarrier, bit and power allocation algorithm for multicell OFDM systems. *Proceedings of IEEE Canadian Conference on Electrical and Computer Engineering CCECE* 2003; **3**: 1531–1534.
8. Xu X, Qiu T, Xu W, He Z, Niu. K. Sub-carrier allocation combined with coordinated multi-point transmission in multi-cell OFDMA system. *Proceedings of IEEE International Conference on Network Infrastructure and Digital Content IC-NIDC* 2009; 842–846.
9. Giuliano R, Monti C, Loreti P. WiMAX fractional frequency reuse for rural environments. *IEEE Transactions on Wireless Communications* 2008; **15**(3): 60–65.
10. Giuliano R, Loreti P, Mazzenga F, Santella G. Fractional frequency reuse planning for WiMAX over frequency selective channels. *Proceedings of IEEE International Wireless Communications and Mobile Computing Conference IWCMC* 2008; 666–671.
11. Hamouda S, Yeh C, Kim J, Shin W, Kwon DS. Dynamic hard fractional frequency reuse for mobile WiMAX.

Proceedings of IEEE Pervasive Computing and Communications PerCom 2009; 1–6.
12. Geirhofer S, Oyman O. Client-centric fractional frequency reuse based on user cooperation in OFDMA networks. *Proceedings of IEEE Conference on Information Sciences and Systems CISS* 2008; 95–100.
13. Geirhofer S, Oyman O. Cooperative fractional frequency reuse based on partial connectivity among clients. *Proceedings of IEEE GLOBECOM* 2008; 1–5.
14. Fujii H, Yoshino H. Theoretical capacity and outage rate of OFDMA cellular system with fractional frequency reuse. *Proceedings of IEEE Vehicular Technology Conference VTC* 2008; 1676–1680.
15. Baum DS, Hansen J, Salo J. An interim channel model for beyond-3G systems: extending the 3GPP spatial channel model (SCM). *Proceedings of IEEE VTC* 2005; **5**: 3132–3136.
16. Choi JG, Bahk S. Cell-throughput analysis of the proportional fair scheduler in the single-cell environment. *IEEE Transactions on Vehicular Technology* 2007; **56**(2): 766–778.
17. Samsung Electronics. Experimental WiBro MCS Table. 2007.

AUTHORS' BIOGRAPHIES

Bumkwi Choi received the B.S. degree in electronic and electrical engineering from Sungkyunkwan University, Suwon, Korea in 2009 and is currently pursuing his M.S. degree in Department of mobile systems engineering at Sungkyunkwan University since March 2009. His research interests include radio resource management and medium access control for 3G/4G and *ad-hoc* networks.

Seyuon Limi received the B.S and M.S. degrees in telecommunication and information engineering from Korea Aerospace University, Goyang, Korea in 2000 and 2002, respectively. Since 2002, he has been working as a Senior Engineer at Telecommunication R&D center in Samsung Electronics and since 2009, he has been also working toward the Ph.D. degree in mobile system engineering from Sungkyunkwan University, Suwon, Korea. His research interests include medium access control and resource allocation for Cognitive Radio network.

Tae-Jin Lee received his B.S. and M.S. in electronics engineering from Yonsei University, Korea in 1989 and 1991, respectively, and the M.S.E. degree in electrical engineering and computer science from University of Michigan, Ann Arbor, in 1995. He received the Ph.D. degree in electrical and computer engineering from the University of Texas, Austin, in May 1999. In 1999, he joined Corporate R&D Center, Samsung Electronics where he was a senior engineer. Since 2001, he has been an Associate Professor in the School of Information and Communication Engineering at Sungkyunkwan University, Korea. He was a visiting professor in Pennsylvania State University from 2007 to 2008. His research interests include performance evaluation, resource allocation, Medium Access Control (MAC), and design of communication networks and systems, wireless MAN/LAN/PAN, home/*ad-hoc*/sensor/RFID networks, next generation wireless communication systems, and optical networks. Since 2004, he has been a voting member of IEEE 802.11 WLAN Working Group, and is a member of IEEE and IEICE.